



Research Article

Automatic Acquisition System for Mine Pressure Monitoring in Coal Mine Working-Face Footage

Miaoer Zhou ¹, Yongkui Shi,¹ Jian Hao,¹ and Xin Chen ²

¹College of Energy and Mining Engineering, Shandong University of Science and Technology, Qingdao 266590, China

²College of Computer Science and Engineering, Shandong University of Science and Technology, Qingdao 266590, China

Correspondence should be addressed to Xin Chen; xxwar@163.com

Received 10 November 2023; Revised 8 January 2024; Accepted 19 January 2024; Published 5 February 2024

Academic Editor: Antonio Lazaro

Copyright © 2024 Miaoer Zhou et al. This is an open access article distributed under the Creative Commons Attribution License, which permits unrestricted use, distribution, and reproduction in any medium, provided the original work is properly cited.

The existing mine pressure monitoring system has realized the online continuous monitoring of the working-face stent resistance, roadway roof offcuts, and anchor rod/rope working resistance. However, the mine pressure monitoring information of the working face currently includes only the stent resistance and the monitoring time, and there is no information on the working-face advance. The mine pressure data cannot be precisely analyzed due to a lack of measurement point locations. Mine pressure data analysis combined with the working-face feed information is the basis for safe and efficient mining and for improving the intelligence level of the comprehensive mining face. According to the special electromagnetic environment of the underground, this system adopts UWB (ultra-wide-band) technology and the SDS-TWR (symmetric double-sided two-way ranging) ranging method, with the UWB positioning base station as the core and installs positioning tags at the end supports of the working face to collect information. The data are uploaded to the host computer via Ethernet for coordinate solving, automatically collecting the working-face footage data and providing positional information for mine pressure monitoring. The application results show that the system operates normally and can collect real-time information of working-face footage and monitor mine pressure data, and meet the requirements of coal mine positioning accuracy, positioning error is less than 30 cm, the application effect is good.

1. Introduction

With the enhancement of domestic energy resource demand, shallow coal mining resources have been unable to meet the display demand, increasing the mining of deep resources yearly. The safety problems in coal production have increasingly triggered the concern of related industries, and Article 114 of the Coal Mine Safety Regulations requires that mining pressure monitoring be carried out in the comprehensive mining face. However, due to the limitations of the production environment [1], technology, and equipment, mine accidents occur frequently in China, with heavy casualties and economic losses. By reviewing the data on the website of the State Administration of Coal Mine Safety Supervision and the publicly available literature, the number of various types of safety production accidents in China's coal mines in the period of 2003–2019 as a percentage of the total number of accidents has been statistically analyzed. The results of the statistical results are shown in Figure 1, in which roof

accidents have the highest frequency of occurrence. The current coal mining process often faces difficulties such as top-coal damage, poor support condition of the stent, and impact load of the team stent, which even destroys coal and rock bodies [2] and causes damage to support equipment, collapse of the roadway, and casualties. Therefore, it is especially important to perform mine pressure monitoring to ensure the support capacity of the stent and to determine the potential safety hazards in coal mines on time.

Scholars at home and abroad have conducted many studies on mine pressure monitoring. Yugay et al. [3] have developed a fiber optic sensor for monitoring pressure variations in mine support elements fiber optic systems will increase the share of mining automation, reduce the share of manual labor, and eliminate measurement errors associated with human factors. Zhou et al. [4] establish a microseismic monitoring system according to the actual needs of the site and to reveal the law of ground pressure manifestation by analyzing the distribution characteristics of microseismic events; to

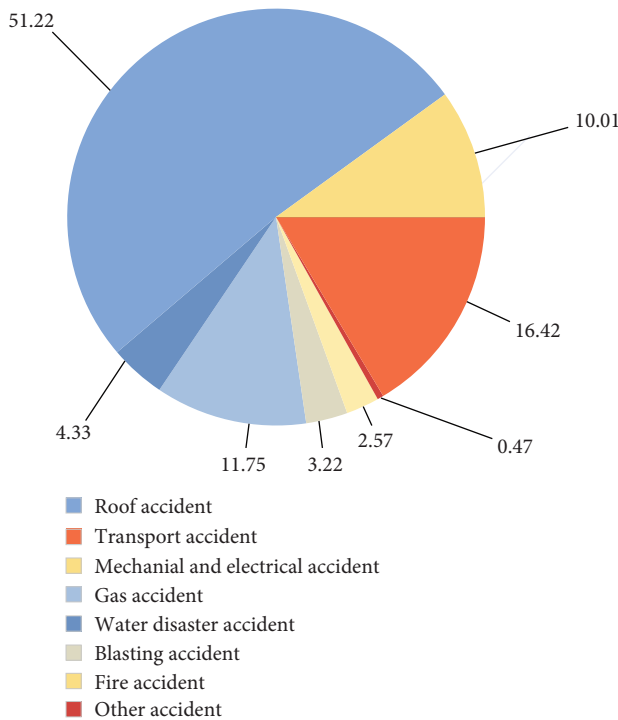


FIGURE 1: Number of accidents of all types in coal mines as a proportion of the total number of accidents.

analyze the occurrence stability of the goaf; further verify it laterally; and finally, demonstrate the feasibility and effectiveness of the microseismic monitoring sensor system. Although in-depth research on mine pressure monitoring and prediction has been carried out at home and abroad, most existing mine pressure monitoring methods are top-plate mine pressure monitoring. Pressure sensors are used in the working face to monitor the change in the working resistance of the hydraulic support. In the coal mine underground monitoring system, the “roof pressure step,” is an important mine pressure early warning parameter, which reflects the regularity of top-plate rupture and movement. Specifically, it refers to the fact that in coal mining, due to the influence of mine pressure, the roof plate will periodically rupture and sink, forming the “incoming pressure”. Each time the “pressure” occurs, the distance the working face advances forward is the “roof pressure step.” This parameter is significant for predicting mine pressure disasters and ensuring mine safety. However, at present, in order to obtain the “roof pressure step,” we can only use the total footage of each shift or each day for average processing; the manual measurement work efficiency is low, and the error of the data obtained is large. Therefore, we need a system that can automatically and accurately measure the working-face footage to improve the accuracy and efficiency of mine pressure monitoring. Combining the monitoring time, measurement point location, footage information, and geological conditions, we can accurately and comprehensively dig out effective information about the pattern of mineral pressure manifestation.

In order to improve the measurement accuracy of the “roof pressure step,” it is necessary to determine the positioning of

the working face and the calculation of the distance between the working face and the footage of the working face based on the monitoring of the mining pressure. Existing positioning technologies applied to the comprehensive mining face in the coal mine mainly include infrared-based positioning technology, inertial navigation-based positioning technology, odometer-based positioning technology, etc. The positioning technology is based on the infrared ray, inertial navigation-based positioning technology, and odometer-based positioning technology.

The infrared-based underground positioning technology installs the infrared-transmitting sensor in the body of the coal mining machine and the infrared-receiving sensor in the hydraulic support [5, 6]. During the digging process, the infrared-transmitting sensor on the body of the coal mining machine continuously sends out infrared pulse signals through directionality, and the infrared-receiving sensor on the corresponding hydraulic support receives the pulse signals and recognizes the position of the coal mining machine relative to the hydraulic support. The infrared-receiving sensor on the corresponding hydraulic support receives the pulse signal, recognizes the position of the coal miner relative to the hydraulic support, and then calculates the position information of the working face. The infrared-based positioning technology is simple and low-cost; however, the high amounts of dust in the coal mine affect the transmission and reception of infrared signals, the positioning accuracy is limited, and it cannot meet the requirements of the accuracy of positioning in the coal mine.

Underground coal mine positioning technology based on an inertial navigation system was first proposed and researched by foreign research institutes in the 1980s. Reid et al. [7], according to the coal mining characteristics of the coal mining machine in the long-arm comprehensive mining face, installed the inertial navigation system in the body of the coal mining machine to accurately measure the three-dimensional paths of the moving process of the coal mining machine with a long arm, which was successfully designed and applied in production [7]. However, the inertial navigation system, after a while, is often affected by environmental factors and inertial navigation on the original data for many times of integration and differentiation, resulting in the rapid accumulation of positioning errors; the final positioning results produce large errors [8]. Based on the above situation, researchers began to use other auxiliary positioning information to inhibit the accumulation and dispersion of positioning errors in the inertial navigation system. Li et al. [9] and Ralston et al. [10] used the combination of an odometer and inertial navigation system through the collection of velocity or displacement information of the odometer to correct the positioning results of the inertial navigation system. However, the combined positioning system has a large amount of data, slow computation speed, and high cost, which is not applicable to the coal mining face.

In summary, although the underground coal mine positioning technology is improving, most of it is still limited by factors such as cost and positioning accuracy. The ultra-wideband (UWB), as an emerging positioning technology, has the advantages of good reliability and high accuracy compared to the other positioning technologies. Chehri et al. [11] conducted

a feasibility study on underground UWB positioning, solved the initial coordinates of the target node using the least-squares method, used an iterative algorithm to find the target node's position coordinates, and verified the method through simulation and experiments. Yazhou et al. [12] proposed the use of multiple sensors for data acquisition for the underground environment, designed the fusion mechanism, and proposed a reliable classification method based on random forest so that the positioning system could adapt to a variety of harsh tunnel environments in the underground. The simulation results show that the average positioning accuracy of this positioning method is 0.75 m. Chung and Ha [13] introduced an UWB positioning system based on the coal mine underground, proposed a mine personnel localization scheme based on the (time of arrival) TOA model, and verified the rationality and feasibility of the scheme through simulation experiments.

This study introduces a mine-pressure-monitoring-oriented working-face footage automatic-acquisition system, selecting the SDS-TWR ranging algorithm and three-side positioning algorithm suitable for the underground environment of coal mines to obtain the working-face footage information and, at the same time, combine with mining pressure sensors to monitor the pressure of the hydraulic stent of the synthesized mining face to realize the dynamic monitoring of the working face, as well as plotting the distribution matrix of the stent resistance at the working face to monitor the location of the local incoming pressure and calculate the incoming pressure step distance.

2. Overview of Relevant Theories

2.1. Introduction to the UWB Technology. The UWB [14–16] has the characteristic of narrowband pulsed communication without the need for a carrier. The Federal Communications Commission (FCC) defines UWB signaling as shown below:

$$\frac{f_H - f_L}{f_H + f_L} \geq 20\%, \quad (1)$$

or

$$f_H - f_L \geq 500 \text{ MHz}. \quad (2)$$

where f_H corresponds to the upper frequency and f_L corresponds to the lower frequency limit.

UWB technology is characterized by large channel capacity, low-average transmission frequency, strong multipath resolution, strong penetration, and strong anti-interference ability. Based on these characteristics, UWB technology has more obvious advantages than the other wireless positioning technologies when facing complex environments such as rough tunnel walls, narrow tunnels, and electromechanical equipment in underground coal mines. In addition, the accuracy of the UWB positioning technology can reach the centimeter level, which meets the design requirements and improves the accuracy of data, thus providing more reliable data support for mine pressure monitoring.

2.2. UWB Localization Methods. Existing positioning algorithms more widely use a distance-based positioning method; in the distance-based positioning method, using a plurality of fixed-base station nodes for positioning, the base station location coordinates are known. In the positioning process, we first measure the distance between the base station and the tag, set the tag coordinates as an unknown solution, and then, with the base station coordinates of the system of simultaneous equations, solve the system of equations that can be derived from the coordinates of the tag. Specific localization methods include the AOA (angle of arrival) localization method, the time difference of arrival (TDOA) localization method, and the TOA localization method.

The AOA positioning method [17] is performed by measuring the direction of the signal emitted by the signal source or the angle of arrival to achieve positioning; in the commonly used indoor positioning system, it is necessary for two location coordinates of the known positioning base station to be received from the positioning tags of the wireless signals, respectively, in order to measure the relative angle between the positioning base station and the wireless signal. According to the angle of the received UWB signal for the intersection, the positioning base station can be used to determine the location of positioning tags.

The TDOA localization method [18] utilizes the UWB signal arrival time difference for localization. The distance difference can be obtained according to the time difference multiplied by the propagation speed of the UWB signal in the air. Then, the hyperbolic equation can be constructed according to the distance difference. The specific realization process is as follows: first, a reference base station is selected, and the other base stations become subbase stations. Then, the subbase station and the reference base station are used as the focal point. The distance difference between the positioning tag and the two base stations is the distance difference between any point on the hyperbola and the focal point, from which hyperbolic equations can be established. The hyperbolas must intersect at one point, and the intersection point is the position coordinates of the positioning tag.

The TOA [19] is based on the known speed of propagation of the signal and the signal from the launch point to the reception point to receive the time required to achieve the distance measurement method. The TOA is realized as follows. First, the signal-transmitting device transmits a signal containing the signal-transmitting moment t_1 ; then, after the signal-receiving device receives the signal, according to the current clock of the signal-receiving device, the signal arrival moment t_2 is recorded, the signal arrival moment t_2 is used to subtract the signal sending moment t_1 , and the signal transmission time is obtained. The distance d between the signal-transmitting device and the receiving device is obtained according to Equation (3) as follows:

$$d = c \times (t_2 - t_1), \quad (3)$$

where c is the propagation speed of electromagnetic waves in air in the general case, $c = 3.0 \times 10^8 \text{ m/s}$.

The underground coal mine tunnel structure is complex, and the space is closed; the temperature, humidity, dust, and the medium of the tunnel will interfere with and affect the accuracy of underground positioning. In addition, the underground tunnel is surrounded by coal or rocky soil, the wall of the tunnel is very rough, and there are all kinds of communication and other equipment hanging above it. The air inside the tunnel contains gases such as carbon monoxide, gas, etc., plus the movement of people and objects, etc., which will affect the propagation of the UWB signals under such special conditions. The information collected by the receiving end of the signals is in error and ultimately affects the positioning accuracy. There are three main reasons for the errors:

- (1) Synchronization delay differences [20, 21]: As the equipment clocks of the transmitting and receiving equipment cannot be highly synchronized, there is a synchronization delay in the ranging process. The synchronization delay is within 10, and the error can be up to 3,000 m, which can not meet the requirements of accurate positioning in underground coal mines.
- (2) Timing errors [22, 23]: The clock pulses of the transmitting and receiving devices are based on the crystal originals within the devices, which have varying degrees of accuracy, resulting in different frequency offsets between different devices.
- (3) Not line of sight (NLOS) transmission errors [24, 25]: Assuming that the ideal clock frequency of the crystal element is f and the frequency shift of the crystal element is Δf , the timing error in the T time period is as follows:

$$\Delta t = \frac{\Delta f}{f} T. \quad (4)$$

Let the timer inherent error factor e be as follows:

$$e = \frac{\Delta f}{f}. \quad (5)$$

The timing error is as follows:

$$\Delta t = eT. \quad (6)$$

Referring to the IEEE 802.15.4a protocol, the clock frequency offset tolerance of the device is. Under the set conditions, the error caused by the timer frequency offset is more than 150 m, and the ranging error is large.

According to the above introduction of positioning methods, it can be seen that the AOA positioning method is not strong in its anti-interference ability in the NLOS environment and is unsuitable for bending, branching, and tilting the roadway in underground coal mines. The TDOA positioning

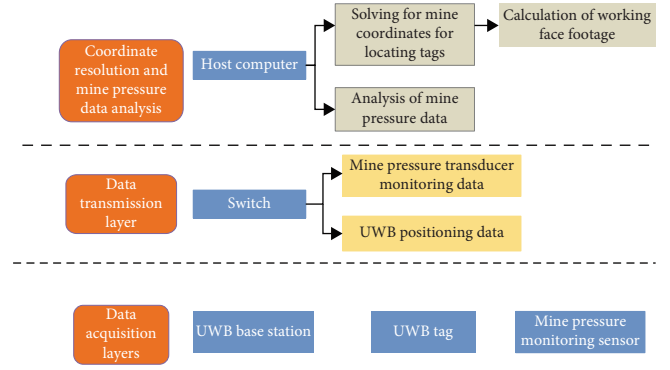


FIGURE 2: Three-story structure plan.

method needs clock synchronization between base stations, and the positioning accuracy is affected by the timing error of the base station. The roadway in underground coal mines is as short as a few dozen meters and as long as several hundred meters; the time of transmission is extended, and it is difficult to realize the synchronization between the base stations. Therefore, TDOA is not suitable to be used for the positioning of the working face of comprehensive mining, and the TOA positioning method is less affected by the environment and does not require clock synchronization between base stations, which reduces the impact of the delayed difference in synchronization and NLOS error on the positioning accuracy; therefore, this study chose the TOA positioning method for determining the positioning of the working face.

3. Design and Realization of an Automatic Acquisition System for Mine Pressure Monitoring in Coal Mine Working-Face Footage

As the application of location-based services in the industrial field becomes more and more widespread, its importance in the underground coal mine, where the environment is complex and changeable, is also becoming more and more prominent. High-precision working-face localization not only helps to collect feed information but can also be combined with the mine pressure monitoring system, which plays a crucial role in guaranteeing the safe production of coal mines. This study comprehensively utilizes UWB, Ethernet, and sensor technology to design a coal mine working-face feed automatic-acquisition system oriented to mine pressure monitoring.

3.1. Overall System Design. The structure of this system is mainly divided into three layers, as shown in Figure 2. The first layer is the data acquisition layer, which consists of a mine pressure monitoring sensor, positioning base station, and positioning tag. First, the UWB tag communicates with the base station to complete the real-time range; the mine pressure monitoring sensor completes the function of collecting the stent resistance data and then sends the data to the second layer. The second layer, the data transmission layer, mainly composed of switches, is responsible for quickly uploading the positioning information and mine

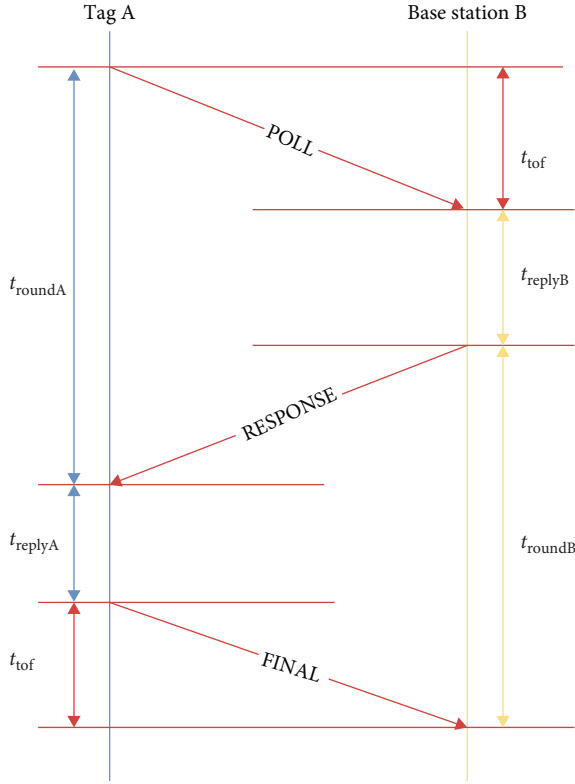


FIGURE 3: Symmetric double-sided two-way ranging.

pressure data collected in the first layer to the host computer via Ethernet. The third layer is the positioning coordinate analysis and mine pressure data analysis layer, which consists of the coordinate analysis host computer that analyzes and calculates the range information and mine pressure data and draws the “dynamic schematic diagram of the working face” and the “matrix diagram of the distribution of the resistance of the working-face support.”

3.2. Calculation Method of Working-Face Footage. This study selects the non-time-synchronized TWR (two-way ranging) ranging method based on the TOA localization method to realize the distance measurement between the base station and the tag. According to the TOA localization method introduced in the previous section, it is known that the essence of UWB ranging is to measure the time of flight of the beacon frame between the tag and the base station. The error caused by clock drift is unavoidable in non-time-synchronized positioning systems. At the same time, the SDS-TWR (symmetric double-sided two-way ranging) ranging method used in this study can sufficiently reduce the ranging error caused by the clock drift. The principle of this ranging method is shown in Figure 3. The SDS-TWR ranging method can be used to measure the distance between the tag and the base station, which can be used in the following way.

The whole range process consists of three communications between the base station and the tags; the first communication is the switching starts timing when tag A sends a POLL packet to base station B. When base station B

receives the packet, the timer stops timing, and the flight time between the tag and the base station is t_{tof} ; the second communication is with a delay of t_{replyB} , base station B sends an acknowledgment RESPONSE packet to tag A [26], the time between sending a packet and receiving it at base station A is t_{roundA} ; the third communication is after t_{replyA} time to reply an answer FINAL packet to the base station B. The time from the transmission of the packet to the receipt of the answer packet by the base station B is t_{roundB} .

The SDS-TWR localization process is shown in Figure 4. Then, according to Figure 3, there is:

$$t_{roundA} = 2t_{tof} + t_{replyB}, \quad (7)$$

$$t_{roundB} = 2t_{tof} + t_{replyA}. \quad (8)$$

From the collation of Equations (7) and (8), the ranging equation of SDS-TWR is given as follows:

$$t_{tof} = \frac{1}{4}(t_{roundA} - t_{replyA} + t_{roundB} - t_{replyB}). \quad (9)$$

Clock drift is expressed as follows:

$$\hat{t}_{roundA} = (1 + e_a)t_{roundA}, \quad (10)$$

$$\hat{t}_{roundB} = (1 + e_b)t_{roundB}, \quad (11)$$

$$\hat{t}_{replyA} = (1 + e_a)t_{replyA}, \quad (12)$$

$$\hat{t}_{replyB} = (1 + e_b)t_{replyB}. \quad (13)$$

From Equations (10)–(13) the estimates are as follows:

$$\begin{aligned} \hat{t}_{tof} &= \frac{1}{4}(\hat{t}_{roundA} - \hat{t}_{replyA} + \hat{t}_{roundB} - \hat{t}_{replyB}) \\ &= \frac{1}{4}((1 + e_a)t_{roundA} - (1 + e_a)t_{replyA} \\ &\quad + (1 + e_b)t_{roundB} - (1 + e_b)t_{replyB}). \end{aligned} \quad (14)$$

According to Equations (9) and (14), the error can be obtained as follows:

$$\hat{t}_{tof} - t_{tof} = \frac{1}{4}((t_{roundA} - t_{replyA})e_a + (t_{roundB} - t_{replyB})e_b). \quad (15)$$

Substituting Equations (7) and (8) into Equation (15) shows:

$$\hat{t}_{tof} - t_{tof} = \frac{1}{2}t_{tof}(e_a + e_b) + \frac{1}{4}(e_a - e_b)(t_{replyB} - t_{replyA}). \quad (16)$$

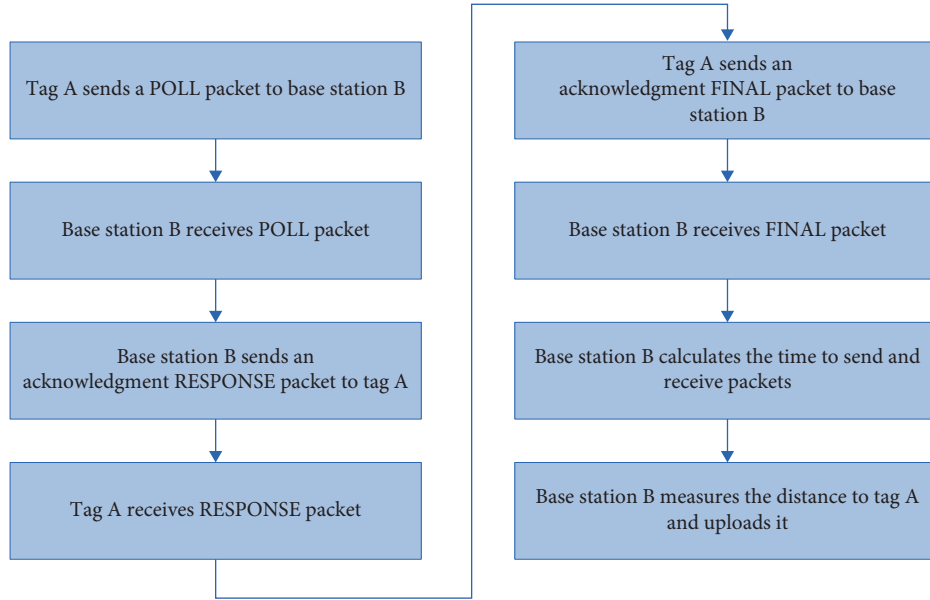


FIGURE 4: SDS-TWR localization process.

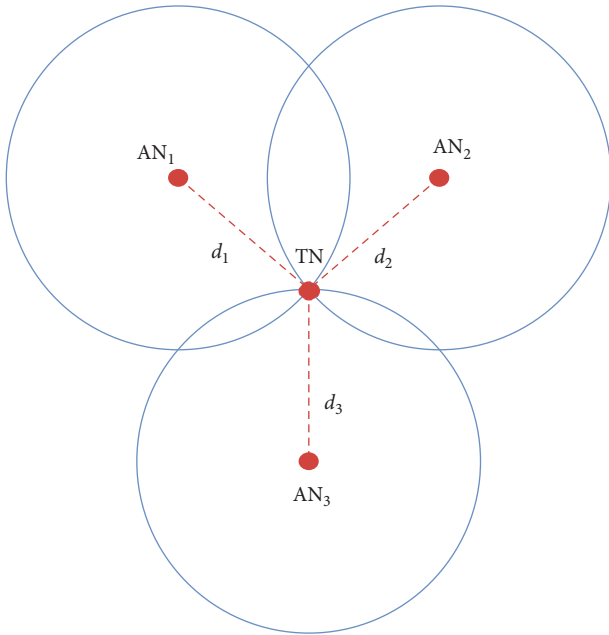


FIGURE 5: Three-side positioning method.

From Equation (16), it follows that when t_{replyB} and t_{replyA} are equal, the timing error $\hat{t}_{\text{tof}} - t_{\text{tof}}$ minimum ensures the system's positioning accuracy.

The step after obtaining the distance between the tag and the base station is to solve the tag position, and one of the more commonly used methods for calculating the coordinates of the tag position is the three-sided localization algorithm [27]; the basic principle is assuming that the tag position is (x, y) , as shown in Figure 5; the respective base station distance from the tag is a radius, drawing three

circles, three base stations measured, and TN distance are d_1, d_2 , and d_3 , respectively, and the intersection location is the location of the tag TN.

The following system of equations is created by solving for the positional coordinates of the tag, i.e., the position of the work surface, using the least-squares method is as follows:

$$\begin{cases} (x_1 - x)^2 + (y_1 - y)^2 = d_1^2 \\ (x_2 - x)^2 + (y_2 - y)^2 = d_2^2 \\ \vdots \\ (x_n - x)^2 + (y_n - y)^2 = d_n^2 \end{cases} \quad (17)$$

Expanding the system of equations and organizing it gives:

$$\begin{cases} x^2 + y^2 + x_1^2 + y_1^2 - 2xx_1 - 2yy_1 = d_1^2 \\ x^2 + y^2 + x_2^2 + y_2^2 - 2xx_2 - 2yy_2 = d_2^2 \\ \vdots \\ x^2 + y^2 + x_n^2 + y_n^2 - 2xx_n - 2yy_n = d_n^2 \end{cases} \quad (18)$$

The above Equation (18) is obtained by using the first equation in the equation and subtracting it sequentially from the last equation in the equation:

$$\begin{cases} x_1^2 - x_n^2 - 2x(x_1 - x_n) - y_1^2 - y_n^2 - 2y(y_1 - y_n) = d_1^2 - d_n^2 \\ x_2^2 - x_n^2 - 2x(x_2 - x_n) - y_2^2 - y_n^2 - 2y(y_2 - y_n) = d_2^2 - d_n^2 \\ \vdots \\ x_{n-1}^2 - x_n^2 - 2x(x_{n-1} - x_n) - y_{n-1}^2 - y_n^2 - 2y(y_{n-1} - y_n) = d_{n-1}^2 - d_n^2 \end{cases} \quad (19)$$

The position coordinate $TN(x, y)$ is calculated using the principle of least squares, viz:

$$X = (A^T A)^{-1} A^T b, \quad (20)$$

where

$$A = -2 \begin{bmatrix} x_1 - x_n & y_1 - y_n \\ x_2 - x_n & y_2 - y_n \\ \vdots & \vdots \\ x_{n-1} - x_n & y_{n-1} - y_n \end{bmatrix}, \quad b = \begin{bmatrix} d_1 - d_n + x_n^2 + y_n^2 - x_1^2 - y_1^2 \\ d_2 - d_n + x_n^2 + y_n^2 - x_2^2 - y_2^2 \\ \vdots \\ d_{n-1} - d_n + x_n^2 + y_n^2 - x_{n-1}^2 - y_{n-1}^2 \end{bmatrix}, \quad X = \begin{bmatrix} x \\ y \end{bmatrix}. \quad (21)$$

According to the SDS-TWR ranging method and the three-sided positioning algorithm, the coordinates of the working surface position can be calculated. With reference to the CGCS2000 geodetic coordinate system, the positions of the base station, tag, and open-cut eye are mapped in the geodetic coordinate system, which is expressed in longitude L , latitude B , and elevation H . The coordinate origin of the CGCS2000 coordinate system is the center of the mass of the earth, the Z -axis points to the CTP as defined by the International Bureau of Time in 1984, and the X -axis is the starting meridian plane and the equatorial plane that passes through the origin and is orthogonal to the Z -axis, which constitutes a right-handed geocentric coordinate system. The geodetic coordinate system is not convenient for calculating the working-face footage, so two-dimensional coordinates in space are chosen.

The geodetic coordinates of the base station are known (L, B, H) , then the spatial 2D coordinates of the tag are calculated according to the following equation (x, y) :

$$\begin{cases} x = (N + H) \cos B \cos L \\ y = (N + H) \cos B \sin L \end{cases}, \quad (22)$$

$$N = \frac{a}{\sqrt{1 - e^2 \sin^2 B}}, \quad (23)$$

$$e^2 = \frac{a^2 - b^2}{a^2}, \quad (24)$$

where N is the radius of curvature of the Uyghur circle; e^2 is the earth's first eccentricity, a is the earth's long semi-axis; and b is the earth's short semi-axis.

In the comprehensive mining face, the coal miner advances along the direction of the roadway and periodically feeds the knife, so the working face is in dynamic change. As the working face advances, the previous area becomes an open area. When the UWB positioning system is used to

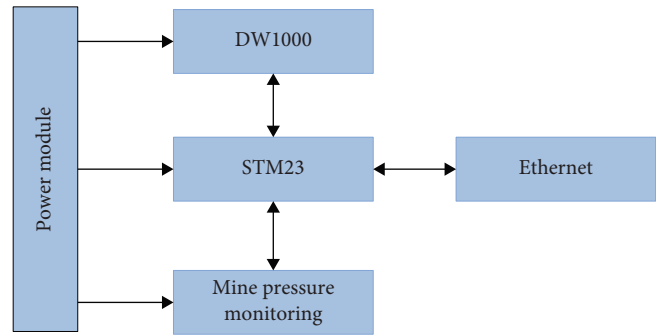


FIGURE 6: The overall framework of the hardware circuit.

locate the working face, UWB base stations and tags are installed in the working-face end supports and working-face tunnels, and the average footage is calculated based on the end supports' left and right footage data.

Since the coordinates of the location of the open-cut eye are known,

$$\text{Workface feed} = |x_{\text{working surface location}} - x_{\text{working face opening position}}|. \quad (25)$$

3.3. System Hardware Design. The overall framework of the hardware of the automatic acquisition system of coal mine working-face advancement designed in this study for mine pressure monitoring is shown in Figure 6.

The hardware circuit includes four main parts, which are the main controller circuit, power supply circuit, DW1000 module circuit, and mine pressure monitoring circuit, and the functions of each part are as follows:

- (1) Power supply circuit: It is mainly responsible for converting the input power supply into a stable 3.3 V DC voltage to provide a stable and reliable power input for the main controller;
- (2) DW1000 module: It is mainly responsible for the communication between modules, recording the timestamp of data frames, and realizing the ranging function. The DW1000 module consists of an SPI bus communicating with the host controller, digital transceiver, analog transmitter, analog receiver, PLL clock, power management, and state controller. The host interface receives the data frame from the external SPI interface, which is processed by the digital transceiver and converted to an analog signal by the analog transmitter, and sends the data through the antenna; during the reception process, the antenna converts the received data by the analog receiver to a digital signal and sends the data to the host interface through the processing of digital transceiver and sends the data through the SPI interface after encapsulation, the encapsulated data frame is sent by SPI interface with timestamp data, from which the distance value measured by the module is calculated;

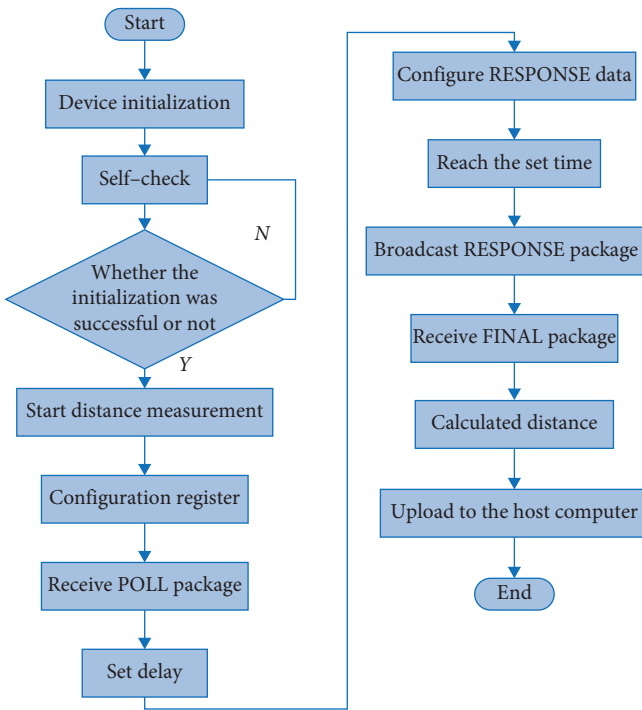


FIGURE 7: UWB base station workflow.

- (3) Main control module: Mainly responsible for obtaining the information of the DW1000 module, calculating the range value, and uploading the range information to the host computer. The system designed in this study uses an STM23F103 chip as the main controller, which is a high-performance 32-bit processor based on Cortex-M3 core design to meet the system design requirements;
- (4) Mine pressure monitoring module: It is mainly responsible for the monitoring of hydraulic support resistance. The pressure sensor of this system is a piezoresistive pressure transmitter, using a monocrystalline silicon chip as the elastic element; monocrystalline silicon material in the role of the force, the resistivity changes, through the measurement circuit, can be obtained proportional to the change in the force of the electrical signal output, and then obtain the hydraulic stent resistance data of the synthesized mining face.

3.4. System Software Design. The software design of this system mainly includes two parts: the embedded software and the host computer software. The embedded software mainly realizes the distance measurement between the base station and the positioning tag and the acquisition of mine pressure data and uploads the distance measurement data and the mine pressure data to the host computer. In contrast, the host computer mainly realizes the drawing of the “working-face advance” and the “matrix of working-face support resistance distribution.”

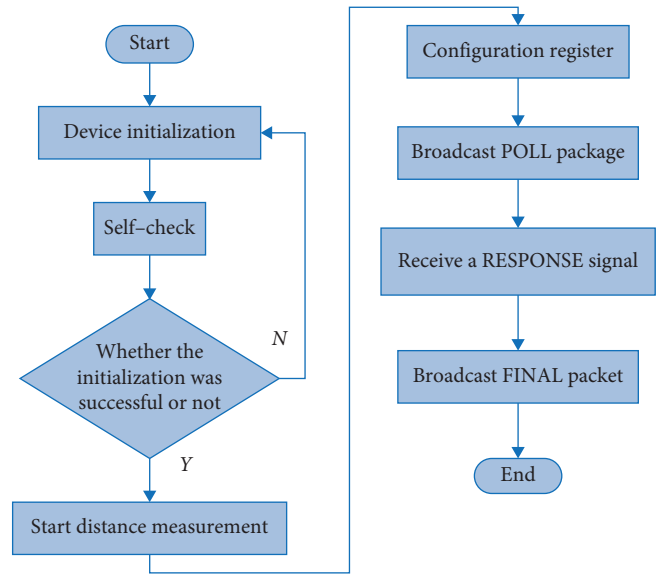


FIGURE 8: Tag workflow.

3.4.1. Embedded Software Design. The embedded software design includes the design of the base station, the positioning tag, and the mine pressure monitoring module, which will be introduced one by one next.

The workflow of the base station is shown in Figure 7. First, the base station initializes each part and performs a power-on self-test, and after successful initialization, it carries out register configuration and sets DW1000 to receive mode. After successfully receiving the POLL message, configure the RESPONSE message, broadcast the RESPONSE packet after a delay, and switch to receive mode, waiting to receive the FINAL from the positioning tag. After receiving the FINAL, the distance between the base station and the positioning tag is calculated according to the SDS-TWR ranging algorithm and uploaded to the supremacy computer, and a ranging cycle ends.

3.4.2. Tag Software Design. The workflow of the tag is shown in Figure 8. As with the base station, the tag starts by initializing and powering up the parts for self-testing. After successful initialization of the tag, DW1000 is configured to transmit mode, broadcasting POLL packets, switching to receive mode after transmission, and then receiving RESPONSE packets from the base station, switching to transmit mode again, broadcasting FINAL packets, and then the end of a ranging cycle.

3.4.3. Mine Pressure Monitoring Module Software Design. The software workflow of the mine pressure monitoring module is shown in Figure 9, where the initialization operation of the module is carried out first, followed by A/D conversion, and finally, the data are uploaded to the host computer through serial communication.

3.5. Host Computer Software Design. The host computer software flow is shown in Figure 10. The host computer first receives the range information from each base station and the mine pressure data collected by the mine pressure sensor;

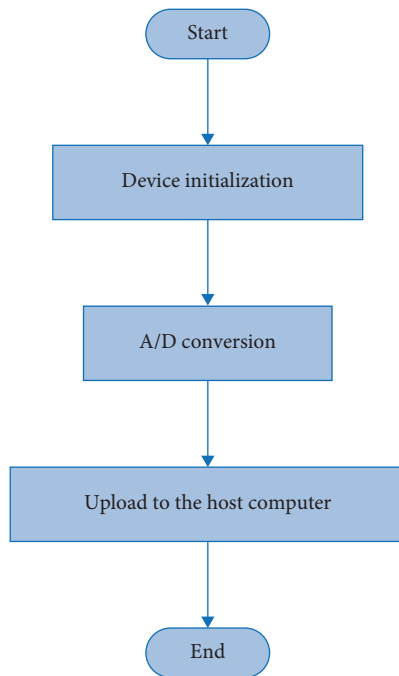


FIGURE 9: Mine pressure monitoring workflow.

then, it solves the position of the positioning tag according to the positioning algorithm introduced in the previous section and then calculates the working-face footage by combining with the coordinates of the open cutting eye of the working-face. Finally, the footage data and mine pressure data are visualized and displayed to realize coal mine safety monitoring.

The system functions mainly include information management, working-face dynamic schematic interface and interface of the working-face stent resistance distribution matrix. The information management function realizes the new creation, viewing, modification, and deletion of work-face information as well as the import of fault information. Using UWB technology to locate the working face, combined with the known mine coordinates to calculate the working-face footage, and provide positional coordinates for the subsequent analysis of mine pressure data. Plotting the working-face stent resistance distribution matrix in the mined area, automatically displaying the areas out of the threshold range in the matrix diagram, and determining the distance between the resistance anomaly areas to provide reference values for the roof movement.

Figure 11 shows the user's new working-face interface. User can create a new work surface in the main interface, after inputting the working-face information, clicking the "save" button will add a new working face to the database, and clicking the "reset" button will clear all the information in the interface text box.

Figure 12 shows the working-face dynamic schematic interface. The interface includes the overview of the working face, fault information, and the distance of the current working face to the fault. Faults are rupture zones of geological structures, and their existence may lead to deformation and

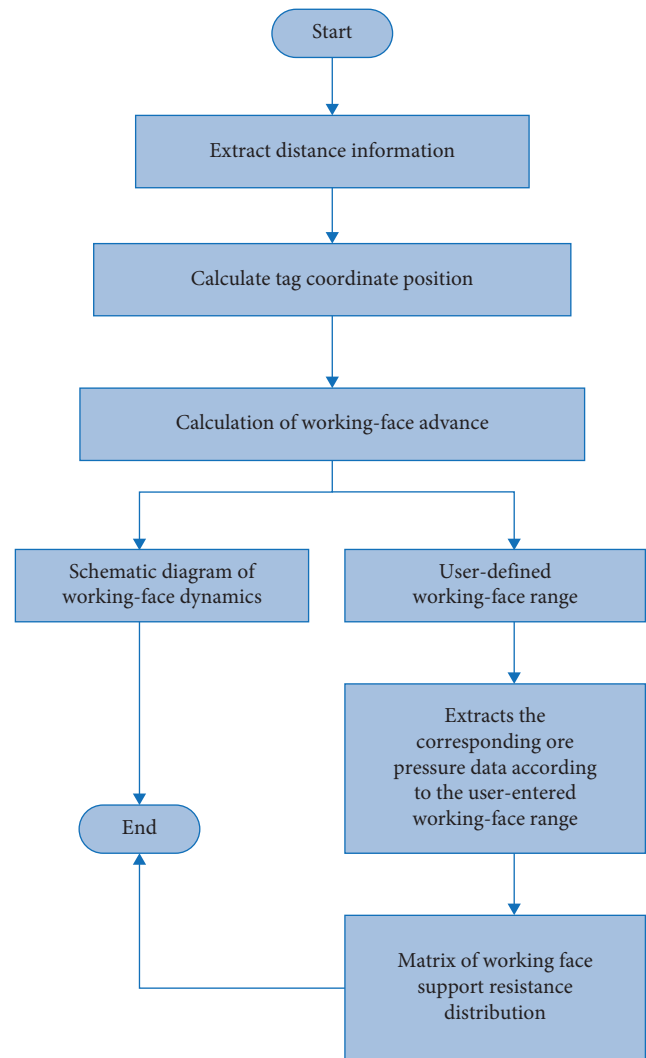


FIGURE 10: Flowchart of the host computer software.

rupture of coal seams and surrounding rocks, increasing the possibility of mine accidents. This system can import known fault information into the system in the form of a database, monitor the distance between the working face and the fault in real time, and take appropriate measures to prevent and control fault-related geologic hazards in order to ensure the safe operation of coal mining.

Figure 13 shows the matrix of working-face support resistance distribution. At the top of the interface are the start of working-face footage, the end of working-face footage, the start sensor number, and the end sensor number, and the matrix square represents the value of the support work resistance of a measurement point at a location. The safety valve opening pressure value determines the color change of the matrix color block, the first digging coefficient, and the second digging coefficient set by the user on the right side of the interface. If the resistance value of the current position is greater than the product of the safety valve opening pressure value and the primary excavation coefficient, the color of the square is red; if the resistance value of the current position is greater than the product of the safety valve

FIGURE 11: New working-face interface. (Note. This figure includes working-face name, coal-seam thickness, microseismic monitoring, roof pressure step, dynamic loading factor of adjacent working faces (the same level) and hydraulic support information).

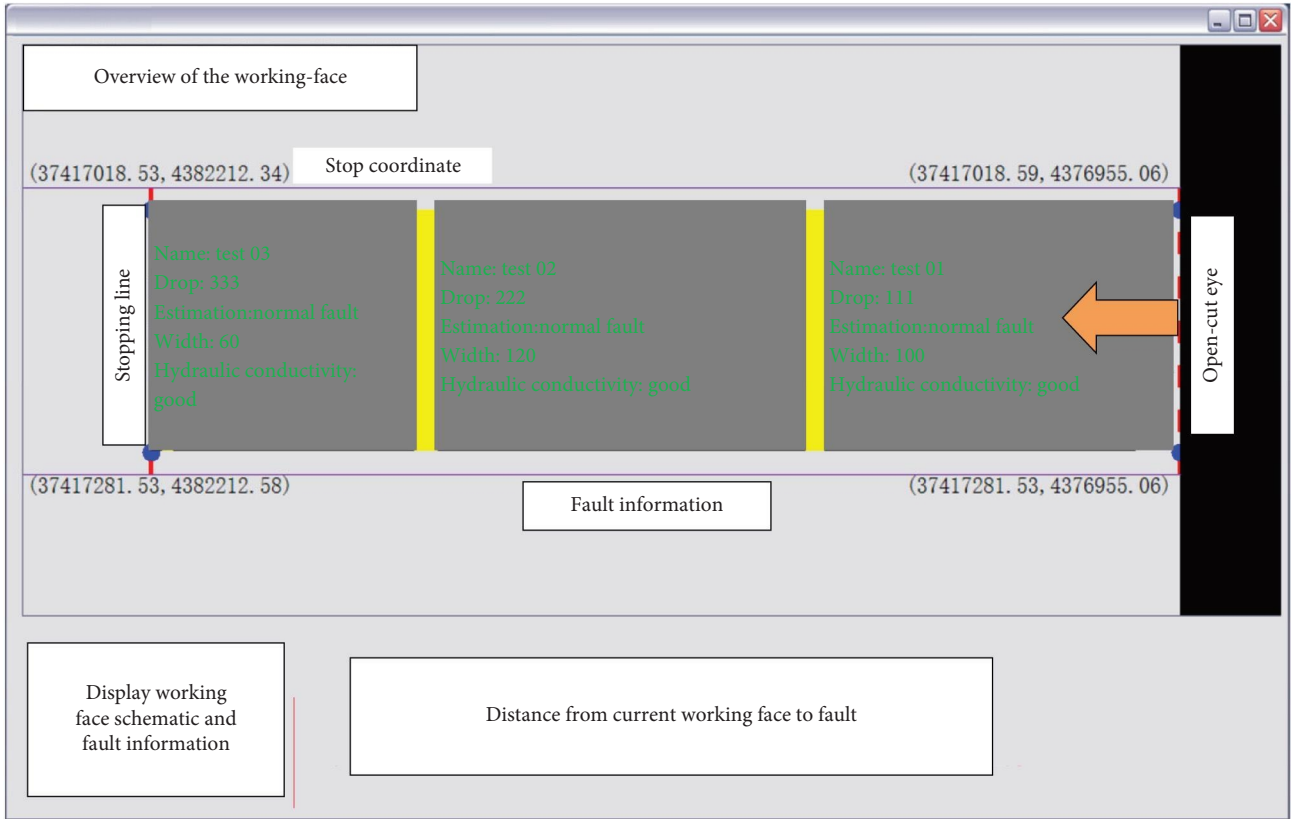


FIGURE 12: Working-face advance.

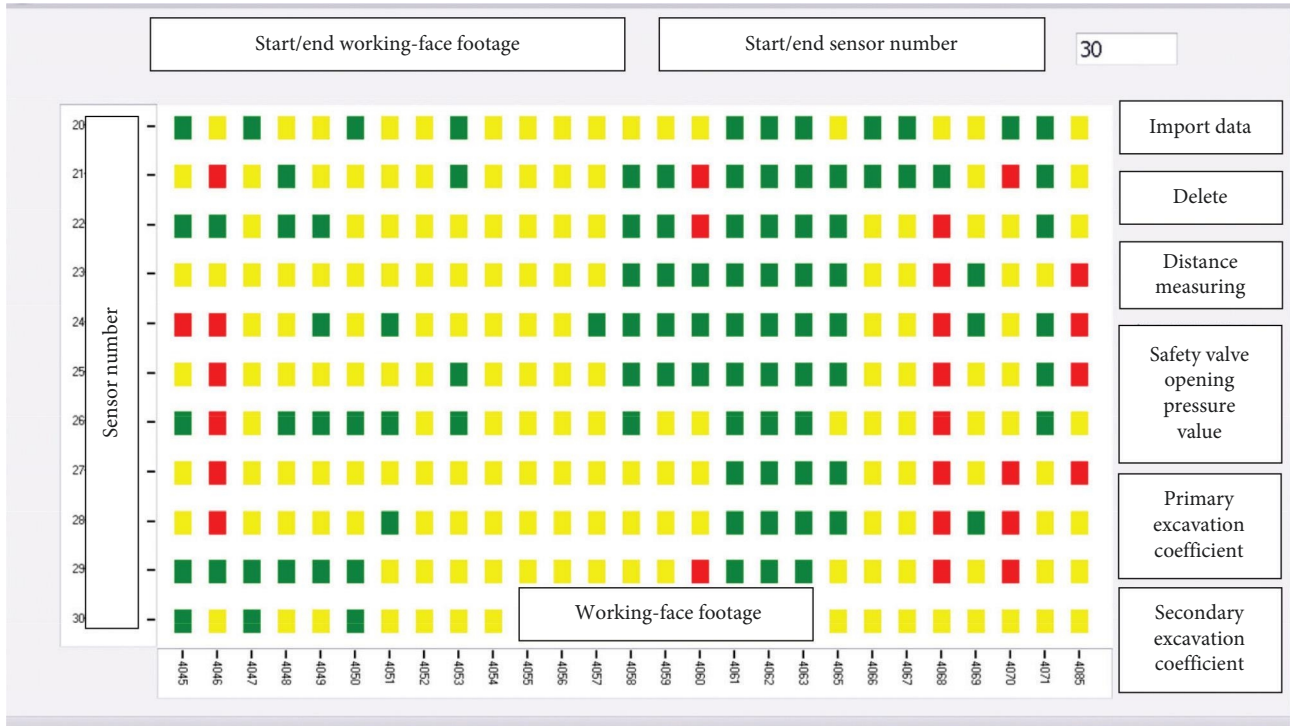


FIGURE 13: Matrix of working-face support resistance distribution.

opening pressure value and the secondary excavation coefficient, the color of the square is yellow; the others are green.

Assuming that at time t_1 , the average working face footage is s_1 , and at time t_2 , the average working face footage is s_2 , and the number of pixels in the horizontal direction of the plotting area is N , the scale of the matrix map is calculated by the formula as follows:

$$sc = \frac{s_2 - s_1}{N}. \quad (26)$$

From Equation 26, the actual distance can be calculated if the number of pixels between two points is measured. For the working face with inconspicuous incoming pressure characteristics, the distance between the abnormal areas of resistance is calculated and determined as the reference value of the roof movement parameters by drawing the distribution matrix of the bracing resistance along the advancing direction of the working face, setting the excavation coefficient, and automatically highlighting the part that exceeds the threshold value in the graph.

4. Engineering Applications

This system is applied to the comprehensive mining face of Dongrong No. 2 Mine to test the UWB-based automatic acquisition system for the working face and verify the applicability and practicality of the system. The system arranges the ground server, the UWB ranging base station, the UWB ranging tags, and mine pressure sensors to monitor the working-face advancement and the resistance of the working-face support.

4.1. Overview of the Working Face. The average strike length of the three faces of the 17th layer under the second south is about 286.2 m, the inclination length is 190.3 m, and the area is 54,463.9 m². The face is located in the lower mining area of South 2, with F65 positive fault in the north, F72 positive fault in the south, unexcavated area above the lower material channel of the second side of the 17th floor in the east, 17th floor -800 in the west, unexcavated area below the contour line, the upper part of the 16th floor three sides of the mining area, with a spacing of about 18 m, and the lower part of the 18th floor one side of the unexcavated area with a spacing of about 15 m.

4.2. Monitoring of Working-Face Progress. The deployment of nodes requires consideration of some of the following factors, as the complex and changing geographic environment of the underground can affect the quality of signal transmission downhole:

- (1) Roughness of the roadway: The rougher it is, the smaller the distance between base stations should be.
- (2) Degree of inclination of the roadway: Appropriately reduce the spacing or add redundant nodes where the inclination is high.
- (3) Roadway length: For shorter roadway, fixed base stations are used, and for longer roadway, removal-migration deployment of the base stations is used.

The underground roadway is roughly strip-shaped, considering the above factors, the deployment of UWB positioning base stations should be visually visible. The spacing of base stations along the length of the roadway is adjusted

TABLE 1: Table of working-face progression.

Name of working face	Time	Footage test values (m)	Actual value of footage (m)	Error (m)
1703	2023-3-1 07:35	46.2	46.2	0.0
1703	2023-3-1 16:32	47.1	47.0	0.1
1703	2023-3-1 18:03	48.0	47.7	0.3
1703	2023-3-1 19:44	48.8	48.5	0.3
1703	2023-3-1 22:25	49.5	49.3	0.2
1703	2023-3-2 02:06	50.4	50.1	0.3
1703	2023-3-2 03:11	51.1	50.8	0.3
1703	2023-3-2 04:36	51.8	51.6	0.2
1703	2023-3-2 05:52	52.5	52.4	0.1
1703	2023-3-2 06:18	53.2	53.2	0.0
1703	2023-3-2 16:50	54.0	54.0	0.0
1703	2023-3-2 18:16	54.6	54.8	0.2
1703	2023-3-2 18:51	55.4	55.3	0.1
1703	2023-3-2 20:06	56.5	56.7	0.2
1703	2023-3-2 23:36	57.3	57.3	0.0
1703	2023-3-3 01:23	58.5	58.3	0.2
1703	2023-3-3 02:27	59.2	59.1	0.1
1703	2023-3-3 03:58	60.1	60.1	0.0
1703	2023-3-3 05:47	60.9	60.9	0.0
1703	2023-3-3 07:21	61.5	61.6	0.1
1703	2023-3-3 14:49	62.3	62.4	0.1
1703	2023-3-3 16:20	63.0	63.1	0.1
1703	2023-3-3 19:45	63.7	63.6	0.1
1703	2023-3-3 20:56	64.5	64.7	0.2
1703	2023-3-4 03:19	65.2	65.2	0.0
1703	2023-3-4 05:51	66.1	66.2	0.1
1703	2023-3-4 07:23	66.6	66.6	0.0
1703	2023-3-4 08:28	67.4	67.2	0.2
1703	2023-3-4 13:46	68.2	68.0	0.2
1703	2023-3-4 16:18	68.9	69.1	0.2
1703	2023-3-4 20:27	69.7	69.8	0.1
1703	2023-3-4 23:02	70.4	70.5	0.1
1703	2023-3-5 02:37	71.2	71.2	0.0
1703	2023-3-5 06:47	71.8	71.5	0.3
1703	2023-3-5 09:38	72.5	72.7	0.2
1703	2023-3-5 11:09	73.8	73.9	0.1
1703	2023-3-5 16:53	74.6	74.6	0.0
1703	2023-3-5 19:22	75.3	75.3	0.0
1703	2023-3-5 22:17	75.8	75.7	0.1
1703	2023-3-5 23:26	76.6	76.5	0.1

accordingly to the actual underground environment, and the spacing between base stations is generally 50–200 m.

In order to verify the applicability and positioning accuracy of the system, the data from March 1, 2023 to March 5, 2023, were selected for analysis. The working-face advance direction was used as the reference to monitor the working-face advance data, and the data table of the working-face advance is shown in Table 1 after the coal miner finished one cut.

The error curve between the test value and the actual value is shown in Figure 14. If the actual value is less than

the test value, the error is negative and if the actual value is greater than the test value, the error is positive.

As shown in Figure 14, the positioning error of the system is less than 30 cm because of the influence of the curvature and inclination of the tunnel in the coal mine and the electromechanical equipment and personnel in the tunnel, etc., which makes the radio signals unable to propagate the LOS (line of sight) directly, and instead propagate the NLOS (not line of sight) through reflections, etc., which generates the NLOS time delay, and thus leads to the measurement error. This error can meet the demand for accurate

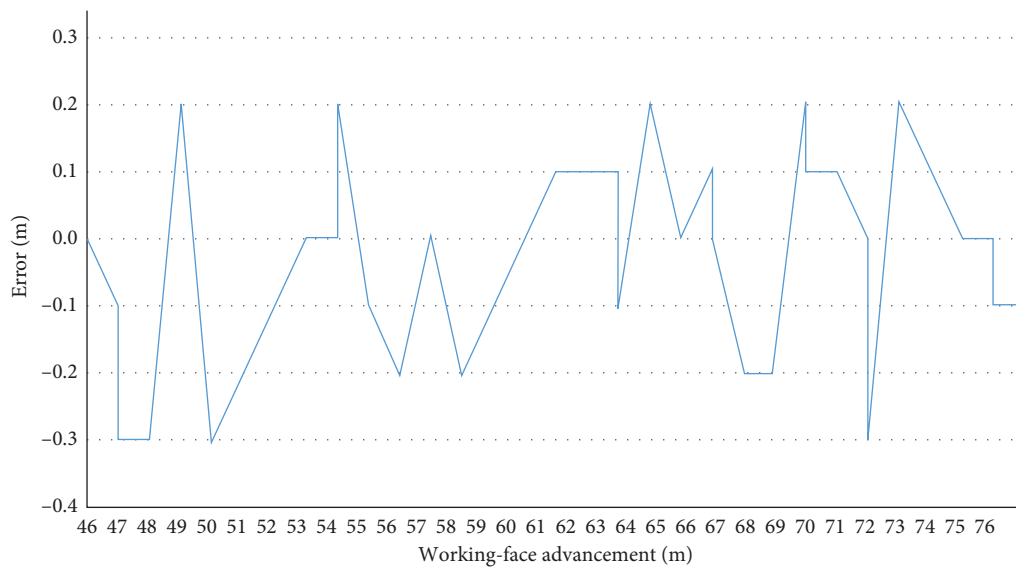


FIGURE 14: Error of working-face advancement.

positioning in the underground environment of a coal mine, so the measurement method of the UWB-based automatic acquisition system of working-face footage is effective and provides a sound data basis for the analysis of mine pressure in the later stage.

5. Conclusion and Next Steps

5.1. Conclusion. This study describes the automatic acquisition system of coal mine working-face advancement for mine pressure monitoring. It carries out the corresponding system structure design according to the special characteristics of the electromagnetic environment underground, thus realizing the dynamic sensing of the working-face position. It solves the problem of the traditional mine pressure monitoring information only consisting of bracket resistance and monitoring time but not the location of measurement points and issues with parameters, such as the fact that the “roof pressure step” can only be measured manually. The construction of a mine pressure dynamic monitoring system in the working face realizes the digitalization and networking of mine pressure monitoring in the roadway of the coal mine working face and meets the requirements of safe production and automatic mine pressure observation in the coal mine working face.

5.2. Next Steps

- (1) Using machine learning and deep learning methods, we analyze the mine pressure data, establish a mine pressure manifestation prediction model, and form an intelligent working-face mine pressure prediction system;
- (2) At the same time, combined with the needs of coal mine safety production, we designed the coal mine safety early warning monitoring platform system, including coal mine underground gas monitoring, microseismic monitoring [28], and fault early

warning monitoring, and integrate the working-face footage collection and mine pressure monitoring into the coal mine safety early warning monitoring platform system to realize data integration.

Data Availability

The data used to support the findings of this study are available from the corresponding author upon request.

Conflicts of Interest

The authors declare that they have no known competing financial interests or personal relationships that could have appeared to influence the work reported in this paper.

Authors' Contributions

The manuscript was written through contributions of all authors. All authors have given approval to the final version of the manuscript.

Acknowledgments

This research was funded by the National Natural Science Foundation of China, grant number 52174121.

References

- [1] H. M. Liu, X. L. Li, Z. Y. Yu et al., “Influence of hole diameter on mechanical properties and stability of granite rock surrounding tunnels,” *Physics of Fluids*, vol. 35, no. 6, Article ID 064121, 2023.
- [2] H. Li, X. Li, J. Fu, Z. Gao, P. Chen, and Z. Zhang, “Research on acoustic emission multi-parameter characteristics in the failure process of imitation steel fiber reinforced concrete,” *Physics of Fluids*, vol. 35, no. 10, Article ID 107109, 2023.
- [3] V. Yugay, A. Mekhtiyev, P. Madi et al., “Fiber-optic system for monitoring pressure changes on mine support elements,” *Sensors*, vol. 22, no. 5, Article ID 1735, 2022.

- [4] Z. Zhou, Y. Huang, and C. Zhao, "Distribution law of mine ground pressure via a microseismic sensor system," *Minerals*, vol. 13, no. 5, Article ID 649, 2023.
- [5] A. Harter, A. Hopper, P. Steggle, A. Ward, and P. Webster, "The anatomy of a context-aware application," *Wireless Networks*, vol. 8, no. 2/3, pp. 187–197, 2002.
- [6] N. B. Priyantha, A. Chakraborty, and H. Balakrishnan, "The cricket location support system," in *6th ACM International Conference on Mobile Computing and Networking*, pp. 32–43, Association for Computing Machinery, Boston, 2000.
- [7] D. C. Reid, D. W. Hainsworth, J. C. Ralston, and R. J. McPhee, "Shearer guidance: a major advance in longwall mining," in *Field and Service Robotics*, S. Yuta, H. Asama, E. Prassler, T. Tsubouchi, and S. Thrun, Eds., vol. 24 of *Springer Tracts in Advanced Robotics*, pp. 469–476, Springer, Berlin, Heidelberg, 2003.
- [8] S. L. Han, X. Y. Ren, J. Z. Lu, and J. Dong, "An orientation navigation approach based on ins and odometer integration for underground unmanned excavating machine," *IEEE Transactions on Vehicular Technology*, vol. 69, no. 10, pp. 10772–10786, 2020.
- [9] H. Li, X. Li, J. Fu et al., "Experimental study on compressive behavior and failure characteristics of imitation steel fiber concrete under uniaxial load imitation steel fiber concrete under uniaxial load," *Construction and Building Materials*, vol. 399, no. 8, Article ID 132599, 2023.
- [10] J. Ralston, D. Reid, C. Hargrave, and D. Hainsworth, "Sensing for advancing mining automation capability: a review of underground automation technology development," *International Journal of Mining Science and Technology*, vol. 24, no. 3, pp. 305–310, 2014.
- [11] A. Chehri, P. Fortier, and P. M. Tardif, "UWB-based sensor networks for localization in mining environments," *Ad Hoc Networks*, vol. 7, no. 5, pp. 987–1000, 2008.
- [12] Y. Yazhou, S. Xiaoqin, L. Zhixin, L. Yuefeng, and G. Xinpeng, "Approach of personnel location in roadway environment based on multi-sensor fusion and activity classification," *Computer Networks*, vol. 148, pp. 34–45.
- [13] W. C. Chung and D. Ha, "An accurate ultra wideband (UWB) ranging for precision asset location," in *IEEE Conference on Ultra Wideband Systems and Technologies*, pp. 389–393, IEEE, USA, 2003.
- [14] E. Martín-Gorostiza, M. A. García-Garrido, D. Pizarro, D. Salido-Monzú, and P. Torres, "An indoor positioning approach based on fusion of cameras and infrared sensors," *Sensors*, vol. 19, no. 11, Article ID 2519, 2019.
- [15] M. Mittelbach, R. Moorfeld, and A. Finger, "Performance of a multiband impulse radio UWB architecture," in *Proceedings of the 3rd International Conference on Mobile Technology, Applications & Systems*, pp. 1–6, Mobility, 2006.
- [16] A. R. Jimenez Ruiz and F. Seco Granja, "Comparing Ubisense, BeSpooon, and Deca wave UWB location systems: indoor performance analysis," *IEEE Transactions on Instrumentation and Measurement*, vol. 66, no. 8, pp. 2106–2117, 2017.
- [17] X. Zheng, B. Wang, J. Zhao, and Z. Lv, "High-precision positioning of mine personnel based on wireless pulse technology," *PLOS ONE*, vol. 14, no. 7, Article ID e0220471, 2019.
- [18] M. Ziegler, A. E. Kianfar, T. Hartmann, and E. Clausen, "Development and evaluation of a UWB-based indoor positioning system for underground mine environments," *Mining, Metallurgy & Exploration*, vol. 40, no. 4, pp. 1021–1040, 2023.
- [19] R. Zandian, *Ultra-wideband based indoor localization of mobile nodes in ToA and TDoA configurations*, PhD Thesis, Universität Bielefeld, Bielefeld, 2019.
- [20] Y. Yamaguchi, T. Abe, and T. Sekiguchi, "Experimental study of radio propagation characteristics in an underground street and corridors," *IEEE Transactions on Electromagnetic Compatibility*, vol. 28, no. 3, pp. 148–155, 1986.
- [21] Z. Sun, *Research on the precise location method of underground personnel in coal mines*, Doctoral dissertation, China University of Mining and Technology, Beijing, 2018.
- [22] A. Wang and Y. Song, "Improved SDS-TWR ranging technology in UWB positioning," in *2018 International Conference on Sensor Networks and Signal Processing (SNSP)*, pp. 222–225, IEEE, China, 2018.
- [23] C. Lian Sang, M. Adams, T. Hörmann, M. Hesse, M. Pörmann, and U. Rückert, "Numerical and experimental evaluation of error estimation for two-way ranging methods," *Sensors*, vol. 19, no. 3, Article ID 616, 2019.
- [24] A. Liu, S. Lin, J. Wang, and X. Kong, "A method for non-line of sight identification and delay correction for UWB indoor positioning," in *2022 IEEE 17th Conference on Industrial Electronics and Applications (ICIEA)*, pp. 9–14, IEEE, Chengdu, China, 2022.
- [25] D.-H. Kim, G.-R. Kwon, J.-Y. Pyun, and J.-W. Kim, "NLOS identification in UWB channel for indoor positioning," in *15th IEEE Annual Consumer Communications & Networking Conference (CCNC)*, pp. 1–4, IEEE, Las Vegas, NV, USA, 2018.
- [26] D. Wang, R. Kannan, L. Wei, and B. Tay, "Time of flight based two way ranging for real time locating systems," in *2010 IEEE Conference on Robotics, Automation and Mechatronics*, pp. 199–205, IEEE, Singapore, 2010.
- [27] G. Ning, W. Zhi-gang, and S. Ke-gang, "Research on indoor positioning algorithm based on trilateral positioning and taylor series expansion," in *Proceedings of 2016 International Conference on Computational Modeling, Simulation and Applied Mathematics (CMSAM 2016)*, pp. 294–299, D E Stech Publications, 2016.
- [28] X. L. Li, D. Y. Chen, J. H. Fu, S. M. Liu, and X. S. Geng, "Construction and application of fuzzy comprehensive evaluation model for rockburst based on microseismic monitoring," *Applied Science*, vol. 13, no. 21, Article ID 12013, 2023.